Chemistry & Biology *13*, 149–159, February 2006 DOI 10.1016/j.chembiol.2005.11.005

Impact of Carbamylation on Type I Collagen Conformational Structure and Its Ability to Activate Human Polymorphonuclear Neutrophils

Stéphane Jaisson,[1] Sandrine Lorimier,[2] Sylvie Ricard-Blum,[3,5] Ganesh D. Sockalingum,[4] Céline Delevallée-Forte,[1] Gregory Kegelaer,[4] Michel Manfait,[4] Roselyne Garnotel,[1] and Philippe Gillery[1,*]

[1] Laboratory of Medical Biochemistry and Molecular Biology
Centre National de la Recherche Scientifique
Unité Mixte de Recherche 6198
Faculty of Medicine
[2] Laboratory of Biomaterials
Institut National de la Santé et de la Recherche Médicale
Equipe de Recherche Mixte 0203
Faculty of Odontology
Institut Fédératif de Recherche 53 Biomolecules
University of Reims Champagne-Ardenne
51095 Reims
France
[3] Institut de Biologie Structurale, Unité Mixte de Recherche 5075
Commissariat à l'Energie Atomique
Centre National de la Recherche Scientifique
Université Joseph Fourier
38000 Grenoble
France
[4] Unité MEDIAN
Centre National de la Recherche Scientifique
Unité Mixte de Recherche 6142
Faculty of Pharmacy
Institut Fédératif de Recherche 53 Biomolecules
University of Reims Champagne-Champagne-Ardenne
51095 Reims
France

Summary

Carbamylation by urea-derived cyanate is a posttranslational modification of proteins increasing during chronic renal insufficiency, which alters structural and functional properties of proteins and modifies their interactions with cells. We report here the major structural alterations of type I collagen induced by carbamylation. Biophysical methods revealed that carbamylated collagen retained its triple-helical structure, but that slight changes destabilized some regions within the triple helix and decreased its ability to polymerize into normal fibrils. These changes were associated with the incapacity of carbamylated collagen to stimulate polymorphonuclear neutrophil oxidative functions. This process involved their interaction with LFA-1 integrin, but no subsequent p^{125}FAK phosphorylation. Carbamylation of collagen might alter interactions between collagen and inflammatory cells in vivo and interfere with the normal remodeling of extracellular matrix, thus participating in the pathophysiological processes occurring during renal insufficiency.

*Correspondence: pgillery@chu-reims.fr
[5] Present address: Institut de Biologie et Chimie des Protéines, Unité Mixte de Recherche 5086, Centre National de la Recherche Scientifique, Université Claude Bernard Lyon, 69008 Lyon, France.

Introduction

Under several pathophysiological conditions, proteins of living organisms undergo posttranslational modifications, which occur throughout their lifespan in vivo and are due to the nonenzymatic binding of various low molecular weight molecules to NH_2 groups of proteins [1]. A well-known posttranslational process is glycoxidation, which increases in diabetes mellitus and is involved in the development of long-term complications of the disease [2–5]. Another, more recently identified posttranslational modification of proteins is carbamylation, which occurs at a higher level during chronic renal insufficiency. The spontaneous formation of cyanate from urea increases as renal function of uremic patients decreases [6, 7]. The active form of cyanate, isocyanic acid, acts as a potential toxin and interacts with NH_2 groups of proteins, and particularly with ϵ-NH_2 groups of lysine residues, generating ϵ-amino-carbamyl-lysine (homocitrulline) [6, 8], as illustrated below:

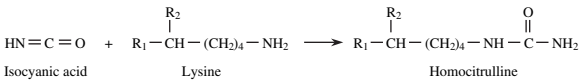

The binding of isocyanic acid to NH_2 groups of proteins can induce conformational changes by affecting the overall charge distribution of the protein, leading to the loss of protein function [6]. For example, many enzymes, like matrix metalloproteinase (MMP)-2 or 6-phospho-D-glucuronate dehydrogenase, exhibit an inhibition of their enzymatic activity after carbamylation [9, 10]. In the same way, both immunological and biological activities of insulin are altered after carbamylation [11]. In this process, a single-residue modification can be sufficient to impair protein function. Indeed, tissue inhibitor of metalloproteinase (TIMP)-2 carbamylated on the α-amino group of the NH_2-terminal cysteine loses its inhibitory activity [12]. Carbamylation of α-crystallins also plays an important role in the development of cataract by generating conformational changes that lead to lens opacity [1, 13]. Furthermore, carbamylation of circulating proteins and hemoglobin has been well-demonstrated in renal insufficiency [14, 15]. These findings underline the role of in vivo carbamylation of proteins in various diseases.

Extracellular matrix (ECM) proteins, including type I collagen, represent preferential targets for cumulative posttranslational modifications, because of their long half-life [6, 9]. Indeed, the carbamylation of ECM proteins in kidneys of uremic patients has been evidenced, by using specific antibodies against homocitrulline [9]. As many cellular functions, such as cell adhesion, cell migration, and protein expression, are controlled by

A **Content of homocitrulline in carbamylated collagen**

	Number of Residues per 1,000[a]	
Collagen	Lysine	Homocitrulline
Control	26.1 ± 0.8	n.d.
2 h-carbamylation	24.6 ± 0.5	1.0 ± 0.2
6 h-carbamylation	21.8 ± 0.6	3.9 ± 0.1
24 h-carbamylation	14.7 ± 0.3	11.2 ± 0.6

[a] Values are means ± standard deviation (n = 3) calculated from complete amino acid analysis of each preparation of collagen. n.d.: not detectable.

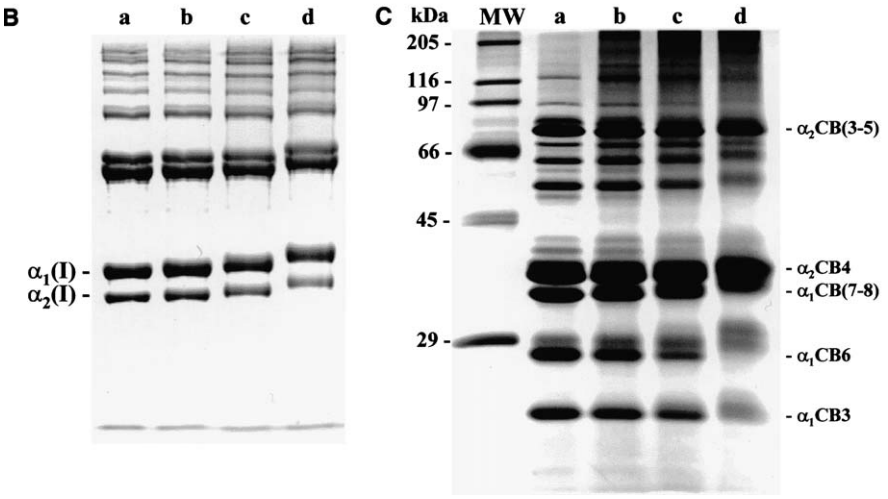

Figure 1. Biochemical Characteristics of Carbamylated Collagen

(A) Measurement of homocitrulline content in several preparations of carbamylated collagen.

(B) SDS-PAGE of carbamylated collagen: 5 μg of (a) control, (b) 2, (c) 6, and (d) 24 hr-carbamylated collagens were analyzed on 5% polyacrylamide gels under reducing conditions.

(C) SDS-PAGE of collagen-derived CNBr peptides: 50 μg of CNBr peptides prepared from (a) control, (b) 2, (c) 6, and (d) 24 hr-carbamylated collagens were analyzed on 12.5% polyacrylamide gels under reducing conditions. MW = standard high molecular weight markers.

interactions between cells and ECM [16–19], carbamylation-induced collagen modifications may alter these interactions and, in this way, dysregulate cell functions. This hypothesis is supported by our previous findings, showing that carbamylated type I collagen selectively regulates metabolic functions of human monocytes, favoring their adhesion and the release of MMP-9 [20].

Moreover, we have previously demonstrated that type I collagen interacted with LFA-1 integrin at the human polymorphonuclear neutrophils (PMNs) membrane and positively regulated PMN respiratory burst, characterized by oxygen free radicals (OFRs) release [21, 22]. Thus, the interaction between these two partners represents a key step in the defense mechanisms against pathogenic agents. Repetition of infections is one of the major causes of morbidity and mortality in uremic patients, but underlying mechanisms have not been clearly elucidated so far [23]. We hypothesize that collagen carbamylation could alter its interaction with PMNs, leading to an impairment of their oxidative functions, and contribute to the increased occurrence of infections during chronic renal insufficiency.

In this study, we investigated, by using biochemical and physical methods, how carbamylation modified the structural and physical properties of collagen and altered its interactions with PMNs.

Results

Amino Acid Analysis of Carbamylated Collagen

Amino acid analysis of the various collagen preparations was carried out by anion exchange chromatography after acid hydrolysis. These analyses showed that carbamylated collagens contained homocitrulline residues, contrarily to control collagen (Figure 1A). Homocitrulline residues were formed from lysine residues, and the number of homocitrulline residues gradually increased with carbamylation time, whereas the number of lysine residues decreased accordingly. After a 2 hr carbamylation, only one lysine residue per 1000 residues (i.e., approximately the size of one α chain of type I collagen) was modified, whereas 4 and 11 residues were converted into homocitrulline when collagen was carbamylated for 6 and 24 hr, respectively.

Electrophoretic Properties of Carbamylated Collagen

Carbamylated collagens were analyzed by 5% sodium dodecyl sulfate-polyacrylamide gel electrophoresis (SDS-PAGE) under reducing conditions. As shown in Figure 1B, carbamylated collagen exhibited characteristic bands of type I collagen, corresponding to α_1(I) and α_2(I) chains. However, α chains of carbamylated collagen migrated more slowly than those of control collagen. The electrophoretic mobility decreased as the duration of carbamylation increased, and was correlated to the number of homocitrulline residues in collagen.

To determine if some of the lysine residues were preferential targets for carbamylation, collagen-derived CNBr-peptides were prepared from carbamylated collagens and analyzed by 12.5% SDS-PAGE. The mobility of CNBr-peptides was differently affected by carbamylation. α_1CB(7-8), α_1CB3, and α_1CB6 peptides exhibited a delayed migration or an enlarged band after 2 or 6 hr of carbamylation, whereas the other peptides (i.e., α_2CB(3-5) and α_2CB4) exhibited differences in their electrophoretic profile after 24 hr only (Figure 1C). These observations showed that lysine residues located in α_1CB(7-8), α_1CB3, and α_1CB6 peptides were the most reactive sites for carbamylation reaction.

Structural Analysis of Carbamylated Collagen by Circular Dichroism and Spectroscopic Methods

As its polyproline II typical structure confers to type I collagen a characteristic circular dichroism (CD) spectrum, carbamylation-induced modifications of collagen structure could be highlighted by using this technique [24]. CD spectra of carbamylated collagens presented the same shape as control collagen, with minimal and maximal values of molar ellipticity at 198 nm and 221 nm, respectively, and a crossover point at 213 nm (Figure 2A). These spectra were consistent with the polyproline II structure of type I collagen, especially the persistence of the 221 nm band, which is used to characterize the helicity of collagen. These results show that carbamylation did not induce the unfolding of the collagen triple helix, although molar ellipticity values of carbamylated collagen were different from those obtained for control collagen, and these differences increased with the duration of the carbamylation process. Indeed, 6 and 24 hr-carbamylated collagens exhibited an increase of the positive band at 221 nm, and a more negative band at 198 nm, in comparison with 2 hr-carbamylated or control collagens (Figure 2A). This change also argued against the possible denaturation of collagen by carbamylation, because the negative peak decreased in denatured collagen [25, 26]. The most pronounced modification occurred between 2 hr and 6 hr of carbamylation. No significant modifications were observed between 6 and 24 hr-carbamylated collagen CD spectra.

Thermal denaturation profiles of control and carbamylated collagens exhibited a sharp transition. The melting temperature (Tm) was found to be 40.8ºC for control collagen, 39.8ºC for 2 hr-carbamylated collagen, and 40.3ºC for 6 hr-carbamylated collagen. These similar values were somewhat higher than the Tm of 24 hr-carbamylated collagen, which was 38.8ºC. According to this result, 24 hr-carbamylated collagen seemed to be less stable in terms of thermal denaturation. Carbamylation did not induce collagen denaturation, but it modified the values of molar ellipticity at 198 and 221 nm, and decreased the denaturation temperature of 24 hr-carbamylated collagen. To investigate these modifications further, control and carbamylated collagens were analyzed by Fourier-transform infrared (FTIR) and Raman spectroscopies.

FTIR and Raman techniques are vibrational spectroscopic methods that provide molecular-level information on the structural composition and environment of the studied sample. The spectra obtained constitute a spectral "fingerprint" that can also be informative of the molecular conformation (e.g., proteins) [27–30]. These techniques are complementary by nature, and they have been applied here to compare control and carbamylated collagens. When FTIR spectra were compared (data not shown), visual inspection only showed very weak differences between the four spectra. However, statistical analysis, allowing comparison of closely related data, demonstrated some subtle differences between the spectra. Distance calculation, based on second derivative spectra in the amide I absorbing region, was performed by using hierarchical cluster analysis based on Ward's algorithm and Euclidean distance calculation. The result of the analysis is represented by a dendrogram, where the distance between spectra is expressed as the heterogeneity value computed from Pearson's correlation coefficient [31]. As can be seen in Figure 2B, FTIR spectra were clustered in two main groups, and a clear differentiation can be made between the 24 hr-carbamylated collagen and the other collagens, the two groups differing in the amide I region. In the second group of spectra, two subgroups can be observed: one corresponding to the 2 and 6 hr-carbamylated collagens, and the other to the control collagen.

The global information obtained after analysis of the FTIR data showing changes in spectral profiles between control and 24 hr-carbamylated collagens led us to complete our investigation by using Raman microspectroscopy, in order to get more insight into the molecular differences between control and carbamylated collagens. For clarity, only two normalized spectra corresponding to control and 24 hr-carbamylated collagen were compared in Figure 2C. Most of the frequency positions remained unchanged or exhibited a few slight shifts. The major band frequencies and tentative assignments are grouped in Table 1. The amide I position corresponding to the C=O stretching mode of the peptide linkage, observed here at 1670 cm^{-1}, for both the control and the 24 hr-carbamylated collagens, indicated that the triple helix conformation was quite well preserved in both samples [29, 30]. The higher amide I intensity of the carbamylated form could reflect the presence of additional C=O groups and/or a closer packing of collagen fibers. The effect of carbamylation was detected on other functional groups, such as the CH_2 deformation at 1450 cm^{-1}, which was more intense and downshifted, suggesting a change in the motion of the lysine CH_2 groups following a change in its length or environment. The protein conformational stability was again visualized by the unchanged position of the amide III bands (1244 and 1269 cm^{-1}) corresponding to NH_2 deformations [27, 28]. The changes observed were only in intensity, not in relative band shift. Fixation of cyanate ions on

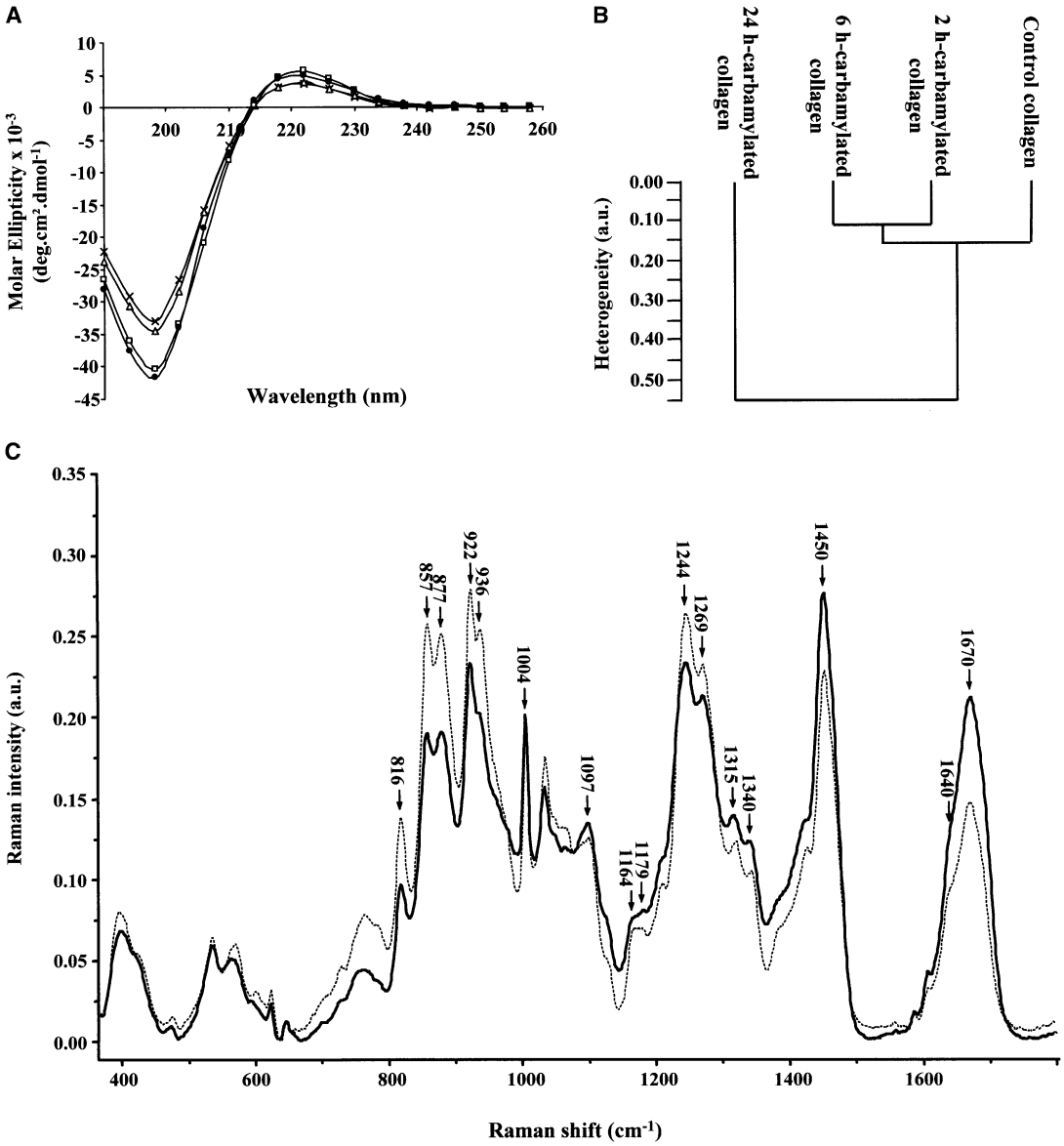

Figure 2. Circular Dichroism and Spectroscopic Analysis of Carbamylated Collagen

(A) CD spectra of control and carbamylated collagen were recorded at room temperature, as described in Experimental Procedures. Symbols: "×"s, control collagen; open triangles, 2 hr-carbamylated collagen; open squares, 6 hr-carbamylated collagen; closed circles, 24 hr-carbamylated collagen.

(B) Representation of the hierarchical clustering of FTIR spectra into groups, corresponding to control, 2, 6, and 24 hr-carbamylated collagens, after statistical analysis performed in the amide I region of second derivative spectra. a.u.: arbitrary units.

(C) Comparison between Raman spectra of control (dotted line) and 24 hr-carbamylated (solid line) collagen. Spectra represent means of three independent measurements and were normalized in the 400–1800 cm^{-1} range.

the lysine residues resulted in a slight increase of the weak shoulders at 1097 and 1122 cm^{-1}, corresponding to CN stretches. Changes in the C-C stretching vibrations of protein backbone and of proline and hydroxyproline rings can be easily observed in the bands situated in the spectral range of 816–936 cm^{-1}, with a change in the relative intensities of the doublets (936/922 and 877/857).

In Vitro Fibrillogenesis of Carbamylated Collagen

Although carbamylation induced only minor changes in collagen structure, we have verified the ability of carbamylated collagens to form fibers under physiological conditions of pH and temperature. Fibrillogenesis of collagen was studied by measuring turbidity at 400 nm, and was characterized by a typical sigmoid curve (Figure 3A). For control collagen, this phenomenon comprised three phases: a lag phase; an exponential phase, which corresponds to the gel assembly; and a plateau, which reflects the stability and density of collagen gels [32, 33]. Fibrillogenesis of carbamylated collagen was characterized by a shorter lag phase, suggesting that carbamylated collagen molecules started to assemble earlier to form fibrils than did control collagen. For 6 and

Table 1. Raman Lines and Their Assignment in Control and 24 hr-Carbamylated Type I Collagen

Control Collagen (cm^{-1})	24 Hr-Carbamylated Collagen (cm^{-1})	Assignment
1670	1670	Amide I ν(C=O)
1640	1640	Amide I ν(C=O)
1606	1606	Phe, Tyr
1586	1586	Pro, Hyp
1452	1450	$\delta(CH_2)$
1425	1423	$\nu(COO^-)$
1342	1340	$\gamma w(CH_2)$
1317	1315	$\gamma t(CH_2)$
1269	1269	Amide III $\delta(NH_2)$
1244	1244	Amide III $\delta(NH_2)$
1208	1206	Hyp, Tyr
1178	1179	NH_3^+
1164	1164	NH_3^+
1125	1122	Protein C-N stretch
1098	1097	ν(C-N)
1062	1062	Bend of carboxyl OH
1046	1046	Not assigned
1033	1031	Phe
1004	1004	Phe
936	936	ν(C-C) of protein backbone
922	922	ν(C-C) of Pro ring
877	877	ν(C-C) of Hyp ring
857	857	ν(C-C) of Pro ring
816	816	ν(C-O-C); ν(C-C) of protein backbone

ν = stretching coordinate; δ = deformation coordinate; γw = wagging coordinate; γt = twisting coordinate; Hyp = hydroxyproline.

24 hr-carbamylated collagen samples, a large decrease in the slope of the exponential phase was noticed, the values reached at the plateau being five times lower than those obtained with 2 hr-carbamylated or control collagen preparations. This suggests that the kinetics of fibril formation were slower for carbamylated collagens than for control collagen, resulting in a variation of gel density due to a decrease in the number of fibers. To complete these data and to assess their robustness, collagen gels formed as described above were submitted to a gradual increase in temperature. The plateau, characteristic of the gel stability, was followed by a rapid decrease in turbidity, corresponding to a progressive gel disruption (Figure 3B). Tm was used to characterize this phenomenon, and was found similar for control and 2 hr-carbamylated collagen gels (46.5ºC and 46.0ºC, respectively). As also indicated by the in vitro fibrillogenesis assay, the major alteration occurred between 2 and 6 hr of carbamylation, since Tm of 6 and 24 hr-carbamylated collagen gels were significantly decreased, being 41.5ºC and 41.0ºC, respectively. These experiments showed that a 6 hr-carbamylation, which modifies only 4 residues in the whole α_1(I) collagen chain, induced a significant alteration of collagen fibrillogenesis, associated with a lower thermostability of the collagen gel.

Scanning Electron Microscopy of Carbamylated Collagen

As those findings could be related to a modification of collagen fiber size or organization, control and carbamylated collagens were further characterized by scanning electron microscopy (SEM). SEM showed that a 2 hr carbamylation did not alter the fiber structure nor the organization of type I collagen network in comparison with control collagen (Figures 4A and 4B). However, an increased carbamylation time induced a progressive modification of fibers, which was more pronounced after

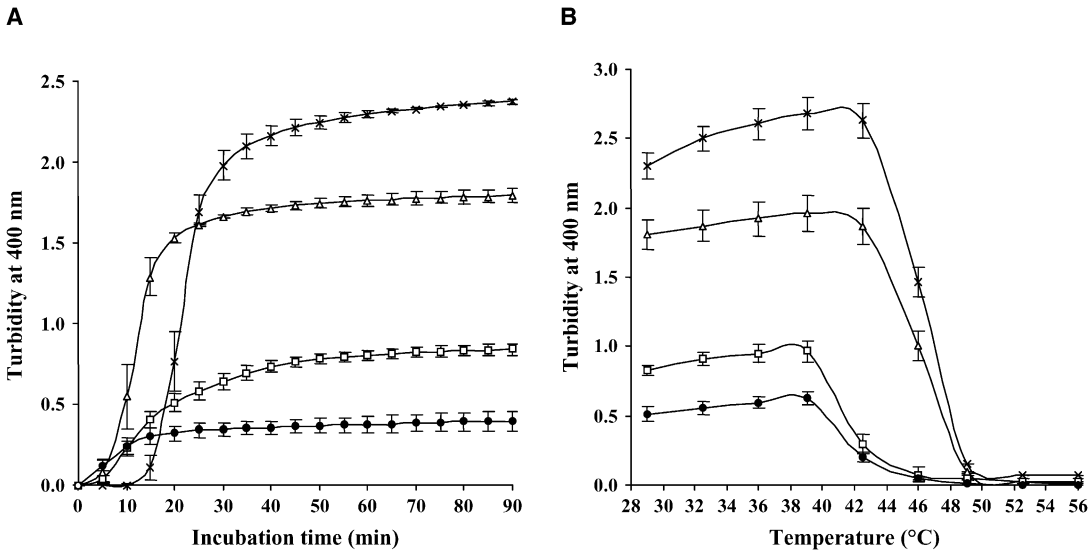

Figure 3. In Vitro Fibrillogenesis of Carbamylated Collagen

(A) Collagen preparations (1 mg/ml in 0.018 M acetic acid) were incubated at 30ºC in phosphate buffer (pH 7.4) for 90 min and turbidity at 400 nm was regularly measured to monitor the fibrillogenesis process. Symbols: "×"s, control collagen; open triangles, 2 hr-carbamylated collagen; open squares, 6 hr-carbamylated collagen; closed circles, 24 hr-carbamylated collagen. Values are means ± standard deviation (n = 3).

(B) Collagen gels were submitted to a gradual increase in temperature, and gel fusion was followed by turbidity measurement at 400 nm. Symbols: "×"s, control collagen; open triangles, 2 hr-carbamylated collagen; open squares, 6 hr-carbamylated collagen; closed circles, 24 hr-carbamylated collagen. Values are means ± standard deviation (n = 3).

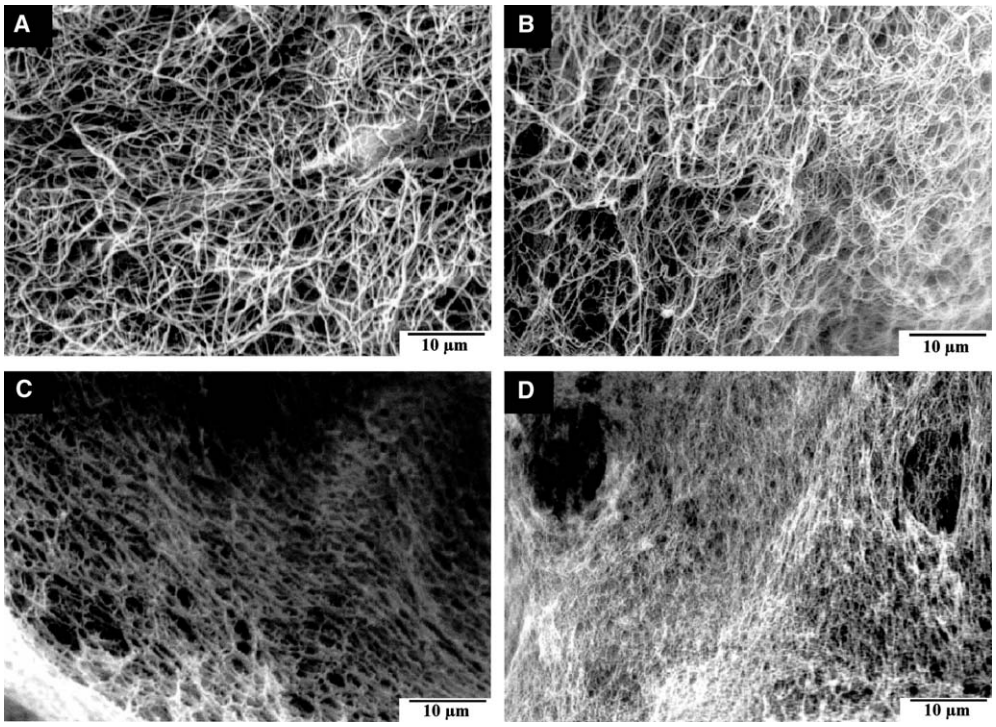

Figure 4. Morphological Aspect of Carbamylated Collagen Fibrils by Scanning Electron Microscopy

Lyophilized collagen was prepared for scanning electron microscopy observation, as described in Experimental Procedures. (A) Control collagen; (B) 2 hr-carbamylated collagen; (C) 6 hr-carbamylated collagen; (D) 24 hr-carbamylated collagen.

6 and 24 hr of treatment (Figures 4C and 4D). The changes observed indicate an association between decrease in the fiber diameter and alteration of the fiber network, which appeared to be more densely packed than control collagen.

Regulation of PMN Functions by Carbamylated Collagen

As structural modifications are usually associated with an alteration of function, we assessed the ability of carbamylated collagen to activate human PMNs. SEM analysis of PMNs after 2 hr of contact with control collagen showed a typical activation state with multiple membrane vesicles involved in the exocytosis process. By contrast, PMNs exhibited generally a uniform and smooth plasma membrane after contact with carbamylated collagen, reflecting the lack of activation (Figure 5A). Using two different methods to quantify OFR production by PMNs (intracellular reduction of nitroblue tetrazolium [NBT] and luminol-dependent chemiluminescence reaction), we showed that carbamylated collagen was far less efficient in activating PMNs than control collagen. The measurement of OFR production by NBT reduction reaction revealed that control collagen induced a significant activation of PMNs (Figure 5B). When PMNs were incubated on carbamylated collagen, OFR production was significantly decreased ($p < 0.01$) in a carbamylation rate-dependent manner (−29% and −45% for 2 and 6 hr-carbamylated collagen, and −67% for 24 hr-carbamylated collagen). A similar inhibition rate was obtained when OFR production was assayed by chemiluminescence test: inhibition percentages reached −24, −36, and −70% for 2, 6, and 24 hr-carbamylated collagens, respectively (Figure 5C). The inhibition of OFR production was associated with a decreased degranulation, evidenced by measurement of elastase and N-acetyl-βD-glucosaminidase release upon PMN activation (see Table S1). In addition, whereas preincubation of PMNs with control collagen significantly increased the f-Met-Leu-Phe-induced production of OFRs, this priming effect was lost when cells were preincubated with carbamylated collagens (Figure S1).

Before exploring the molecular mechanism involved in the inhibition of OFR production, we checked that carbamylated collagen did not alter PMN viability and was unable to directly scavenge OFRs (data not shown). PMN adhesion was not modified on carbamylated collagen, showing that the inhibition of PMN activation was not explained by adhesion impairment (Figure 6A). Previous works of our laboratory have shown that PMN adhesion to type I collagen was mediated by LFA-1 integrin (CD11a/CD18) [21]. This integrin is also involved in PMN adhesion to carbamylated collagen: the number of adherent PMNs was dramatically decreased when cells were preincubated with blocking antibodies raised against CD11a and CD18 subunits, whereas no significant effect was observed in the presence of anti-CD11b and anti-CD11c antibodies (Figure 6A). However, the subsequent transduction pathways were altered by carbamylated collagen. Western blotting analysis showed that control collagen induced focal adhesion kinase (p^{125}FAK) phosphorylation on tyrosine 397, whereas 24 hr-carbamylated collagen was unable to stimulate p^{125}FAK phosphorylation (Figure 6B).

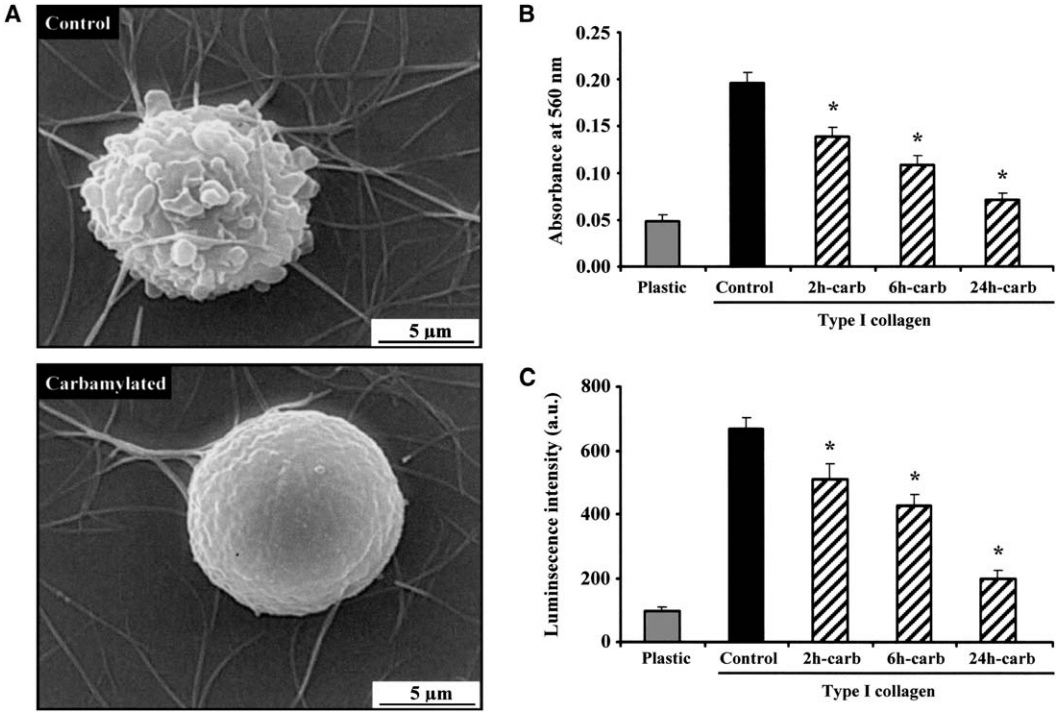

Figure 5. Regulation of PMN Oxidative Functions by Carbamylated Collagen

(A) SEM analysis of PMNs morphology after 2 hr of incubation on control or 6 hr-carbamylated collagen. Measurement of oxygen free radical (OFR) production by PMNs incubated for 2 hr at 37°C on plastic (negative control), or on control, 2, 6, and 24 hr-carbamylated collagens by NBT intracellular reduction assay (B) and by chemiluminescence assay (C), as described in Experimental Procedures. Results are expressed as mean ± standard deviation (n = 3). Significant difference versus control collagen: *p < 0.01. a.u. = arbitrary units.

Discussion

Carbamylation refers to the nonenzymatic reaction of urea-derived cyanate with NH_2 groups of amino acids and proteins, occurring particularly on ϵ-NH_2 groups of lysine residues, thus generating homocitrulline residues. In vivo, this posttranslational modification is a consequence of chronic renal insufficiency, and its intensity increases with urea concentration [6, 7]. Carbamylation of hemoglobin and plasma proteins has been demonstrated in uremic patients [14, 15], and Kraus et al. have found carbamylation of ECM proteins in kidneys of patients with chronic renal insufficiency [9]. Because of their long half-life, it is expected that ECM proteins

A **Adhesion of PMNs on carbamylated collagen: involvement of LFA-1 integrin**

Collagen	No antibodies	Control IgG1	Anti-CD11a	Anti-CD11b	Anti-CD11c	Anti-CD18
Control	0.603 ± 0.020	0.605 ± 0.008 NS	0.351 ± 0.055 **	0. 598 ± 0.061 NS	0.599 ± 0.032 NS	0.105 ± 0.025 **
2h-carbamylation	0.545 ± 0.083	0.583 ± 0.050 NS	0.317 ± 0.044 **	0.601 ± 0.031 NS	0.531 ± 0.075 NS	0.046 ± 0.029 **
6h-carbamylation	0.551 ± 0.056	0.622 ± 0.011 NS	0.281 ± 0.040 **	0.543 ± 0.038 NS	0.573 ± 0.028 NS	0.007 ± 0.072 **
24h-carbamylation	0.548 ± 0.060	0.607 ± 0.008 NS	0.322 ± 0.027 **	0.560 ± 0.078 NS	0.456 ± 0.165 NS	0.051 ± 0.025 **

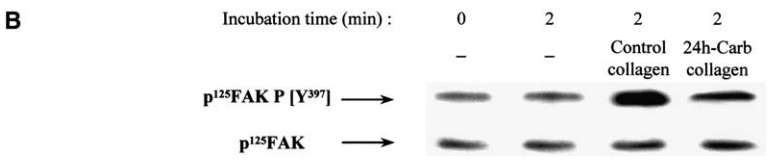

Figure 6. Analysis of PMN Interaction with Carbamylated Collagen

(A) Involvement of LFA-1 integrin in PMN adhesion on carbamylated collagen: PMNs were preincubated with blocking antibodies raised against CD11a, CD11b, CD11c, and CD18, or with control IgG_1 antibody (negative control). PMN adhesion was measured by crystal violet staining after 2 hr of incubation at 37°C on control, 2, 6, or 24 hr-carbamylated collagens. Results are expressed as mean ± standard deviation (n = 3). Significant difference versus control collagen: **p < 0.01; NS = non significant.

(B) Western blotting analysis of the phosphorylation of focal adhesion kinase (p^{125}FAK): PMNs interacted with control or 24 hr-carbamylated collagen for 2 min at 37°C. Western blotting of p^{125}FAK and [Y^{397}]phosphorylated-p^{125}FAK was performed on cell lysates as described in Experimental Procedures.

exhibit greater carbamylation rates than circulating proteins. The changes induced in protein structural features by carbamylation may be involved in pathophysiological processes in vivo [34, 35]. For instance, we have previously shown that carbamylated type I collagen altered monocyte functions, such as adhesion or MMP-9 release [20]. We hypothesized that the effects of collagen carbamylation on monocyte functions could be explained by conformational changes disturbing interactions between collagen and cells.

The aims of this study were, therefore, first to determine carbamylation-induced changes in the structure of type I collagen and, second, to determine if these chemical modifications modified cell-collagen interactions using another type of inflammatory cell, PMNs. Type I collagen was carbamylated in vitro by incubation at 37ºC with 0.1 M KCNO for 2, 6, or 24 hr according to the procedure of Qin et al. [36]. As shown by amino acid analysis, 2, 6, and 24 hr-carbamylated collagens contained, respectively, 1, 4, and 11 homocitrulline residues per 1000. This carbamylation rate was in agreement with that obtained by Shaykh et al. (i.e., 10 per 1000) for carbamylated serum proteins [37].

Although some lysine residues were converted into homocitrulline residues, carbamylated collagen exhibited characteristic α chains, as shown in Figure 1B. However, the electrophoretic migration of α chains of carbamylated collagen was delayed. Such a phenomenon has commonly been observed when collagen is overhydroxylated on lysine residues [38, 39], suggesting that the migration delay is due to structural modifications. Otherwise, Fazili et al. have demonstrated that carbamylation of albumin increased the protein Stokes radius, thus modifying its behavior in size-exclusion chromatography [40]. We performed cyanogen bromide digestion of carbamylated collagen to determine the localization of modified lysine residues. Electrophoretic mobilities of the α_1CB(7–8) and α_1CB6 peptides, and of α_1CB3 peptide to a lesser extent, were decreased by carbamylation. This suggests that the lysine residues initially modified by carbamylation were located within the α_1 chain. This might have a more pronounced effect on the structure of the type I collagen molecule, which contains two α_1 chains and one α_2 chain, than the carbamylation of the α_2 chain. However, it is not known if the two α_1 chains of a given collagen molecule can be simultaneously carbamylated or not. We tried to localize modified lysine residues by analyzing the primary sequence of modified CNBr-peptides. Although α_1CB(7–8), α_1CB6, and α_1CB3 peptides contain 22, 6, and 5 lysine residues, respectively, several of those residues are found in a Gly-X-Lys sequence, which makes them potential targets for hydroxylation. Since cyanate does not react with hydroxylated lysine residues, there are only six lysine residues in the α_1CB(7–8) peptide and three residues in both α_1CB6 and α_1CB3 peptides, which could be preferentially carbamylated. α_1CB6 and α_1CB3 peptides contain the same number of lysine residues, which are potentially able to react with cyanate, but the α_1CB3 peptide seems to be modified to a lesser extent than the α_1CB6 peptide, according to changes in its electrophoretic mobility after carbamylation. Thus, the extent of carbamylation is not directly related to the number of lysine residues within a sequence, and other factors, such as accessibility, are likely to participate in the targeting of lysine residues for modification. Although carbamylation is a nonenzymatic process, it does not affect lysine residues at random within the collagen molecule. This is also the case for nonenzymatic glycation, another nonenzymatic modification of collagen [2], which shows preferential sites on both α_1CB3 and α_2CB(3–5) peptides in rat tail tendon collagen [41]. In contrast, all the lysine residues can be carbamylated readily, although at different rates, in αA-crystallin [36], but not in αII-crystallin, where the N-terminal glycine is the main site of carbamylation [42].

As our preliminary results suggested conformational modifications, we analyzed structural characteristics of carbamylated collagen by different methods, first by CD. CD studies have already been used to highlight carbamylation-induced conformational changes in hemoglobin or bovine α-crystallin [34, 35]. The spectra obtained from control or carbamylated collagens were of similar shape, with minimum and maximum at 198 nm and 221 nm, respectively, and a crossover point at 213 nm. These results are in agreement with characteristic values reported in the literature [24, 43]. The triple helical structure of all samples was assessed by the presence in the spectra of the positive band at 221 nm, which is lost during collagen denaturation [25, 43]. However, intensities at the positive and negative bands were modified proportionally with carbamylation rate. According to Bhatnagar and Gough, this could reflect a conformational change in triple helical polymers [24]. Carbamylation for up to 6 hr did not induce a significant change in Tm. In contrast, molecules carbamylated for a longer period of time exhibited a decreased Tm, suggesting that the presence of 11 homocitrulline residues induced local destabilization of the triple helical structure.

To better characterize its structural changes, carbamylated collagen was analyzed by FTIR and Raman spectroscopic methods. Spectral information obtained from the protein region, amide I and II (FTIR data) and amide I and III (Raman data), suggested that the triple helix was slightly modified upon carbamylation [27, 29, 30]. Although very weak, the differences in the amide I absorption region, highlighted by the second derivative FTIR spectra, distinguished the control and carbamylated forms by statistical analysis. In the Raman spectra, the stable position of the amide I band at 1670 cm^{-1} (C=O stretching mode, triple helical structure) indicated the absence of strong hydrogen bonding. The existence of two amide III lines at 1244 and 1269 cm^{-1} (NH_2 deformation modes), in both control and carbamylated collagens, suggested that both forms could have polar (low proline content) and nonpolar (high proline content) regions coexisting in the chain [27]. The change in relative intensities of the C-C stretching modes of proline and hydroxyproline, observed in the Raman spectra, would suggest that slight changes in these two secondary amino acids occurred upon carbamylation.

We further investigated the impact of carbamylation on the specific ability of collagen to undergo spontaneous assembly. In vitro fibrillogenesis experiments showed that carbamylation induced a progressive loss of collagen ability to form fibrils. Delorenzi et al. reported observing such a fibrillogenesis defect when type I collagen was incubated in the presence of monovalent

anions, such as SCN^- [44]. Conversion of lysine residues in homocitrulline and changes in proline and hydroxyproline detected by Raman spectroscopy could disturb interactions between collagen molecules and their quarter-stagger assembly, thus preventing the regular growth of fibrils. In vivo, it is expected that the presence of carbamylated collagen would impair the incorporation of newly synthetized collagen molecules, eventually leading to a general disorganization of the fibrillar structure of the tissue. The measurement of Tm of carbamylated collagen gels is in agreement with this hypothesis, carbamylated collagen gels being more prone to temperature denaturation than control collagen gels. As fibrillogenesis defect is usually associated with a decreased diameter in fibers [39, 44], carbamylated collagen was analyzed by SEM. SEM observation of carbamylated collagen showed that the fiber network was more densely packed and was comprised of thinner fibers than control collagen. These modifications suggest that the changes induced by carbamylation within the triple helix disturbed the lateral packing of collagen molecules, probably because of an increased steric hindrance.

Considering previous works of our laboratory demonstrating the role of collagen as a modulator of leukocyte functions [21, 22, 45], we tested the ability of carbamylated collagen to activate human PMNs, since uremic patients usually exhibit a defect in PMN functions [23]. Our results demonstrated that the production of OFRS by PMNs was strongly inhibited when collagen was modified by carbamylation. Such effects were not due to a decreased adhesion of PMNs on carbamylated collagen, since no significant differences were observed in adhesion assay. As a matter of fact, the contact of PMNs with carbamylated collagen involved LFA-1 integrin, as in the case of control collagen. However, carbamylation inhibited further interactions between PMN membrane proteins and the carbamylated sequence, as evidenced by the inhibition of p^{125}FAK phosphorylation, the first step responsible for the activation of intracellular pathways leading to phosphorylation of NADPH oxidase subunits.

The inhibition of PMN stimulation was clearly dependent on the intensity of carbamylation, a significant effect being noticed in preparations of collagen containing a single residue of homocitrulline. These results led us to hypothesize that carbamylation takes place preferentially on lysine residues located near the specific sequence DGGRYY, required for the activation of PMNs and contained in the α_1CB6 peptide, as previously shown in our laboratory [22]. This hypothesis is supported by the fact that α_1CB6 peptide is one of the sequences that theoretically possess the most reactive carbamylation sites and that this peptide is indeed a preferential target for carbamylation. The carbamylation of such a lysine residue could generate localized conformational disorders, interfering with the secondary structure of the activating sequence, and could be sufficient to impair the stimulating effect of this sequence on PMNs.

In conclusion, carbamylation does not induce major alterations of collagen structure (only 1% of the total number of residues is transformed under our conditions, which is consistent with in vivo carbamylation rate), in contrast to glycoxidation, another important posttranslational modification, which generates stable crosslinks between proteins. However, the minor changes induced by carbamylation and detected by CD, FTIR, and Raman spectroscopy lead to a decreased thermal stability and to an impaired ability of carbamylated collagen to promote extensive fibrillogenesis. These structural modifications are concomitant with the loss of collagen ability to activate PMNs, which could be a contributing factor in the development of pathophysiological processes during chronic renal insufficiency (e.g., infectious states).

Significance

Carbamylation is a posttranslational chemical modification caused by the nonenzymatic reaction of cyanate, a by-product of urea, with free NH_2 groups, especially with lysine residues of proteins. Posttranslational modifications are known to induce alterations in structural and functional properties of proteins and to modify their interactions with cells. In this article, we report the impact of carbamylation on structural and functional characteristics of type I collagen. This collagen plays a crucial role in connective tissue architecture, and is involved in leukocyte activation, a key event in host defense mechanisms. During chronic renal insufficiency (a pathological state that enhances the carbamylation reaction because of increased urea concentration), patients exhibit repeated inflammatory and infectious disorders incompletely explained by classical causes. Here, we show that carbamylation of less than 1% of collagen amino acids leads to an impaired ability of carbamylated collagen molecules to promote fibrillogenesis and to a decreased thermal stability. In addition to these alterations, carbamylated collagen loses its capacity to stimulate oxidative functions of polymorphonuclear neutrophils, via a signaling pathway involving LFA-1 integrin and focal adhesion kinase (p^{125}FAK). These events may contribute to the complications observed in chronic renal insufficiency. Indeed, the impaired ability of carbamylated collagen to promote fibrillogenesis could induce a disorganization of extracellular matrix and alter its turnover in tissues such as vessel walls and kidneys. Furthermore, its impaired ability to stimulate PMN functions could participate in the development of inflammatory syndromes and infections, which are the major causes of morbidity and mortality in uremic patients.

Experimental Procedures

Chemicals

All chemicals were obtained from Sigma (St. Louis, MO), unless otherwise mentioned.

Preparation of Carbamylated Collagen

Acid-soluble type I collagen was prepared from Sprague-Dawley rat tail tendons by acetic acid extraction [45], and carbamylated by incubation with 0.1 M KCNO in 0.15 M phosphate buffer (pH 7.4), for 2, 6, or 24 hr at 37°C [36]. Control series were prepared by incubating collagen in the same buffer containing 0.1 M KCl in place of KCNO. Collagen was then extensively dialyzed against distilled water until no potassium could be detected by flame photometry (Chiron Diagnostics, Model 480). Subsequently, collagen was lyophilized and solubilized at 2 mg/ml in 0.018 M acetic acid. To evaluate the number

of homocitrulline residues generated by carbamylation, 400 μg of carbamylated collagen were hydrolyzed in 6 M HCl for 18 hr at 110ºC. Analysis of amino acid composition was performed by anion exchange chromatography (Hitachi 880 analyzer, Roche Diagnostics).

Electrophoretic Mobility of Carbamylated Collagen and CNBr-Peptides

Carbamylated and control CNBr peptides were prepared as described by Epstein et al. [46]. Briefly, collagen solubilized at 10 mg/ml in 70% (v/v) formic acid was incubated under N_2 for 4 hr at 30ºC in the presence of an excess of CNBr. CNBr peptides were then lyophilized and dissolved in distilled water at a concentration of 4 mg/ml.

Collagen samples were reduced by 3% (v/v) 2-mercaptoethanol and denatured by heating for 3 min at 90ºC. Electrophoresis of carbamylated collagen and CNBr peptides was performed by SDS-PAGE on 5% or 12.5% polyacrylamide gels. Gels were stained with Coomassie Brillant Blue R250.

Circular Dichroism Analysis

Before CD analysis, collagen was dissolved at 200 μg/ml in 0.05 M acetic acid. CD spectra (190–260 nm) were recorded with a CD 6 spectrometer (Jobin-Yvon, Horiba, France) at room temperature in a quartz cell with a path length of 1 mm. Two spectra were collected for each collagen sample or for 0.05 M acetic acid and were averaged. The spectrum of 0.05 M acetic acid was substracted from the collagen spectra. To record unfolding of the triple helix during denaturation, ellipticity was monitored at 221 nm as a function of temperature. The temperature was increased from 20ºC to 65ºC with a linear gradient of 2ºC/min. The Tm was taken as the point of inflection of the curves.

Raman Microspectroscopy

Raman spectra were recorded directly on the control and on 2, 6, and 24 hr-carbamylated collagen fibers with a commercial Raman microspectrometer (Lab Ram; Jobin-Yvon). The 785 nm radiation from an Ar^+ pumped titanium:sapphire laser (Les Ulis, Spectra Physics, France) was used for excitation. The laser power at the sample was about 80 mW, and other experimental parameters were as follows: grating, 950 gr/mm; 10 acquisitions of 10 s each; confocal hole set to 150 μm. These parameters gave spectra that were measured at a spectral resolution of 6 cm^{-1} and spatial resolution of a few microns. These conditions were kept constant for all the measurements. Raman data were recorded in the 400–1800 cm^{-1} spectral range, and spectral treatment was carried out with the LabSpec 4.04 software (Jobin-Yvon).

FTIR Spectroscopy

FTIR spectra of control, 2, 6, and 24 hr-carbamylated collagens were recorded in the solid form as thin pellets by using transmission mode. The thin pellets were prepared by mixing about 0.5–1.0 mg of collagen with 100 mg of KBr and pressed into thin discs at 10,000–15,000 psi. The resultant sample appears as a thin, transparent film with a spectrum corresponding to an absorbance value between 0.00 and 0.35 arbitrary units. The FTIR instrument used was an Equinox 55 spectrometer (Wissenbourg, Bruker Optics, France) equipped with a KBr beamsplitter and a DTGS detector. Spectra were acquired between 4000–400 cm^{-1} at 64 scans and 4 cm^{-1} resolution with OPUS NT software (Bruker Optics). Data treatment (cluster analysis) was performed by using the IDENT package of OPUS NT.

In Vitro Fibrillogenesis Assay

To study the effect of carbamylation on fibrillogenesis, 0.5 ml of control or carbamylated collagen solution (at 1 mg/ml in 0.018 M acetic acid) was mixed with an equal volume of 0.15 M phosphate buffer (pH 7.4), and transferred to the cell compartment of a Beckman DU640B spectrophotometer (Beckman, Villepinte, France), maintained at 30ºC by water circulation. Fibrillogenesis was monitored by recording absorbance at 400 nm as a function of time. Absorbance was converted into turbidity by multiplying by a factor of 2.303 [47]. Collagen that had been previously denatured by heating for 30 min at 60ºC was used as negative control of fibrillogenesis.

Measurement of Collagen Gel Tm

Collagen solution was mixed with an equal volume of 0.15 M phosphate buffer (pH 7.4) as described above for the in vitro fibrillogenesis assay, and incubated for 90 min at 30ºC to obtain collagen gel. Temperature was then gradually increased up to 56ºC (+0.5ºC/min), and turbidity at 400 nm was regularly measured. Gel melting was characterized by the temperature corresponding to one half of maximal turbidity.

Scanning Electron Microscopy

Lyophilized collagen was fixed in situ with 2.5% (w/v) glutaraldehyde in phosphate-buffered saline (PBS; pH 7.4) for 1 hr at 4ºC. After three washings in PBS, collagen was frozen in liquid nitrogen and broken to reveal its inner structure. For the study of PMN morphologic modifications after contact with collagen, cells were previously incubated for 2 hr at 37ºC in Dulbecco's solution (0.137 M NaCl, 0.0027 M KCl, 0.03 M Hepes, 0.01 M Glucose, 0.0013 M $CaCl_2$, 0.001 M $MgCl_2$, [pH 7.4]). All samples were then dehydrated in graded ethanol followed by graded acetone/ethanol solutions, to pure acetone, further dessicated with a critical-point dryer [48], and coated with palladium-gold (Ion Sputter IFC 1100; Jeol, Croissy sur Seine, France). The observations were carried out with a scanning electron microscope (JSM 5400 LV; Jeol).

Regulation of PMN Functions by Carbamylated Collagen

All the experimental procedures used to characterize the regulation of PMN functions by carbamylated collagen have been fully detailed in the Supplemental Data.

Statistical Analysis

All experiments requiring statistical analysis were performed in triplicate and the results expressed as means ± standard deviation. Significance of differences was calculated by using the Student's t test.

Supplemental Data

Supplemental Data, including Figure S1 and Table S1, are available at http://www.chembiol.com/cgi/content/full/13/2/149/DC1/.

Acknowledgments

The authors thank Alain Malgras and François Chastang for amino acids analysis, C. Murali Krishna for technical assistance with Raman microspectroscopy analysis, and Mireille Dumoulin for fitting CD data.

Received: March 24, 2005
Revised: October 31, 2005
Accepted: November 8, 2005
Published: February 24, 2006

References

1. Harding, J.J., Beswick, H.T., Ajiboye, R., Huby, R., Blakytny, R., and Rixon, K.C. (1989). Non-enzymic post-translational modification of proteins in aging: a review. Mech. Ageing Dev. *50*, 7–16.
2. Fu, M.X., Wells-Knecht, K.J., Blackledge, J.A., Lyons, T.J., Thorpe, S.R., and Baynes, J.W. (1994). Glycation, glycoxidation, and cross-linking of collagen by glucose: kinetics, mechanisms, and inhibition of the late stages of the Maillard reaction. Diabetes *43*, 676–683.
3. Paul, R.G., and Bailey, A.J. (1996). Glycation of collagen: the basis of its central role in the late complications of ageing and diabetes. Int. J. Biochem. Cell Biol. *28*, 1297–1310.
4. Brownlee, M., Vlassara, H., and Cerami, A. (1984). Nonenzymatic glycosylation and the pathogenesis of diabetic complications. Ann. Intern. Med. *101*, 527–537.
5. Vlassara, H. (1997). Recent progress in advanced glycation end products and diabetic complications. Diabetes *46*, S19–S25.
6. Kraus, L.M., and Kraus, A.P. (1998). The search for the uremic toxin: the case for carbamoylation of amino acids and proteins. Wien. Klin. Wochenschr. *110*, 521–530.
7. Kraus, L.M., and Kraus, A.P. (2001). Carbamoylation of amino acids and proteins in uremia. Kidney Int. *78*, S102–S107.

8. Stark, G.R. (1965). Reactions of cyanate with functional groups of proteins: 3. Reactions with amino and carboxyl groups. Biochemistry *4*, 1030–1036.
9. Kraus, L.M., Gaber, L., Handorf, C.R., Marti, H.P., and Kraus, A.P. (2001). Carbamoylation of glomerular and tubular proteins in patients with kidney failure: a potential mechanism of ongoing renal damage. Swiss Med. Wkly. *131*, 139–145.
10. Ganea, E., and Harding, J.J. (1996). Inhibition of 6-phosphogluconate dehydrogenase by carbamylation and protection by alpha-crystallin, a chaperone-like protein. Biochem. Biophys. Res. Commun. *222*, 626–631.
11. Oimomi, M., Hatanaka, H., Yoshimura, Y., Yokono, K., Baba, S., and Taketomi, Y. (1987). Carbamylation of insulin and its biological activity. Nephron *46*, 63–66.
12. Higashi, S., and Miyazaki, K. (1999). Reactive site-modified tissue inhibitor of metalloproteinases-2 inhibits the cell-mediated activation of progelatinase A. J. Biol. Chem. *274*, 10497–10504.
13. Derham, B.K., and Harding, J.J. (2002). Effects of modifications of alpha-crystallin on its chaperone and other properties. Biochem. J. *364*, 711–717.
14. Balion, C.M., Draisey, T.F., and Thibert, R.J. (1998). Carbamylated hemoglobin and carbamylated plasma protein in hemodialyzed patients. Kidney Int. *53*, 488–495.
15. Wynckel, A., Randoux, C., Millart, H., Desroches, C., Gillery, P., Canivet, E., and Chanard, J. (2000). Kinetics of carbamylated haemoglobin in acute renal failure. Nephrol. Dial. Transplant. *15*, 1183–1188.
16. Monboisse, J.C., Rittié, L., Lamfarraj, H., Garnotel, R., and Gillery, P. (2000). In vitro glycoxidation alters the interactions between collagens and human polymorphonuclear leucocytes. Biochem. J. *350*, 777–783.
17. Lefèvre, F., Garnotel, R., Georges, N., and Gillery, P. (2001). Modulation of collagen metabolism by the nucleolar protein fibrillarin. Exp. Cell Res. *271*, 84–93.
18. Lin, C.Q., and Bissell, M.J. (1993). Multi-faceted regulation of cell differentiation by extracellular matrix. FASEB J. *7*, 737–743.
19. Juliano, R.L., and Haskill, S. (1993). Signal transduction from the extracellular matrix. J. Cell Biol. *120*, 577–585.
20. Garnotel, R., Sabbah, N., Jaisson, S., and Gillery, P. (2004). Enhanced activation of and increased production of matrix metalloproteinase-9 by human blood monocytes upon adhering to carbamylated collagen. FEBS Lett. *563*, 13–16.
21. Garnotel, R., Monboisse, J.C., Randoux, A., Haye, B., and Borel, J.P. (1995). The binding of type I collagen to lymphocyte function-associated antigen (LFA) 1 integrin triggers the respiratory burst of human polymorphonuclear neutrophils. J. Biol. Chem. *270*, 27495–27503.
22. Monboisse, J.C., Bellon, G., Randoux, A., Dufer, J., and Borel, J.P. (1990). Activation of human neutrophils by type I collagen: requirement of two different sequences. Biochem. J. *270*, 459–462.
23. Vanholder, R., and Ringoir, S. (1993). Infectious morbidity and defects of phagocytic function in end-stage renal disease: a review. J. Am. Soc. Nephrol. *3*, 1541–1554.
24. Bhatnagar, R.S., and Gough, C.A. (1996). Circular Dichroism and the Conformational Analysis of Biomolecules (New York: Plenum Press).
25. Brown, J.C., Golbick, R., Mann, K., and Timpl, R. (1994). Structure and stability of the triple-helical domains of human collagen XIV. Matrix Biol. *14*, 287–295.
26. Liang, J.N., and Chakrabarti, B. (1981). Spectroscopic studies on pepsin-solubilized vitreous and cartilage collagens. Curr. Eye Res. *1*, 175–181.
27. Parker, F.S. (1983). Applications of Infrared, Raman and Resonance Raman Spectroscopy in Biochemistry (New York: Plenum Press).
28. Juszczak, L.J. (2004). Comparative vibrational spectroscopy of intracellular tau and extracellular collagen I reveals parallels of gelation and fibrillar structure. J. Biol. Chem. *279*, 7395–7404.
29. Badii, F., and Howell, N.K. (2003). Elucidation of the effect of formaldehyde and lipids on frozen stored cod collagen by FT-Raman spectroscopy and differential scanning calorimetry. J. Agric. Food Chem. *51*, 1440–1446.
30. Ikoma, T., Kobayashi, H., Tanaka, J., Walsh, D., and Mann, S. (2003). Physical properties of type I collagen extracted from fish scales of *Pagrus major* and *Oreochromis niloticas*. Int. J. Biol. Macromol. *32*, 199–204.
31. Naumann, D., and Helm, D. (1991). Microbiological characterizations by FT-IR spectroscopy. Nature *351*, 81–82.
32. Holmes, D.F., Capaldi, M.J., and Chapman, J.A. (1986). Reconstitution of collagen fibrils in vitro: the assembly process depends on the initiating procedure. Int. J. Biol. Macromol. *8*, 161–166.
33. Brennan, M., and Davison, P.F. (1980). Role of aldehydes in collagen fibrillogenesis in vitro. Biopolymers *19*, 1861–1873.
34. Simons, E.R., Hartzband, P., Whitin, J., and Chapman, C. (1976). Circular dichroism studies of cyanate-induced conformational changes in hemoglobins A and S. Biochemistry *15*, 4059–4064.
35. Beswick, H.T., and Harding, J.J. (1984). Conformational changes induced in bovine lens alpha-crystallin by carbamylation: relevance to cataract. Biochem. J. *223*, 221–227.
36. Qin, W., Smith, J.B., and Smith, D.L. (1992). Rates of carbamylation of specific lysyl residues in bovine alpha-crystallins. J. Biol. Chem. *267*, 26128–26133.
37. Shaykh, M., Pegoraro, A.A., Mo, W., Arruda, J.A., Dunea, G., and Singh, A.K. (1999). Carbamylated proteins activate glomerular mesangial cells and stimulate collagen deposition. J. Lab. Clin. Med. *133*, 302–308.
38. Hirota, A., Ebihara, T., Kusubata, M., Kobayashi, M., Kobayashi, K., Kuwaba, K., Tanaka, K., Kiriyama, T., Irie, S., and Koyama, Y. (2003). Collagen of chronically inflamed skin is over-modified and upregulates secretion of matrix metalloproteinase 2 and matrix-degrading enzymes by endothelial cells and fibroblasts. J. Invest. Dermatol. *121*, 1317–1325.
39. Torre-Blanco, A., Adachi, E., Hojima, Y., Wootton, J.A., Minor, R.R., and Prockop, D.J. (1992). Temperature-induced post-translational over-modification of type I procollagen: effects of over-modification of the protein on the rate of cleavage by procollagen N-proteinase and on self-assembly of collagen into fibrils. J. Biol. Chem. *267*, 2650–2655.
40. Fazili, K.M., Mir, M.M., and Qasim, M.A. (1993). Changes in protein stability upon chemical modification of lysine residues of bovine serum albumin by different reagents. Biochem. Mol. Biol. Int. *31*, 807–816.
41. Reiser, K.M., Amigable, M.A., and Last, J.A. (1992). Nonenzymatic glycation of type I collagen: the effects of aging on preferential glycation sites. J. Biol. Chem. *267*, 24207–24216.
42. Martin, S., and Harding, J.J. (1989). Site of carbamoylation of bovine gamma-II-crystallin by potassium [^{14}C]cyanate. Biochem. J. *262*, 909–915.
43. Piez, K.A., and Sherman, M.R. (1970). Characterization of the product formed by renaturation of alpha 1–CB2, a small peptide from collagen. Biochemistry *9*, 4129–4133.
44. Delorenzi, N.J., Sculsky, G., and Gatti, C.A. (1996). Effect of monovalent anions on type I collagen fibrillogenesis in vitro. Int. J. Biol. Macromol. *19*, 15–20.
45. Garnotel, R., Rittié, L., Poitevin, S., Monboisse, J.C., Nguyen, P., Potron, G., Maquart, F.X., Randoux, A., and Gillery, P. (2000). Human blood monocytes interact with type I collagen through alpha x beta 2 integrin (CD11c-CD18, gp150–95). J. Immunol. *164*, 5928–5934.
46. Epstein, E.H., Scott, R.D., Miller, E.J., and Piez, K.A. (1971). Isolation and characterization of the peptides derived from soluble human and baboon skin collagen after cyanogen bromide cleavage. J. Biol. Chem. *246*, 1718–1724.
47. Wood, G.C., and Keech, M.K. (1960). The formation of fibrils from collagen solutions: 1. The effect of experimental conditions: kinetic and electron-microscope studies. Biochem. J. *75*, 588–598.
48. Anderson, T.F. (1966). Physical Techniques in Biological Research Second Edition, A.W. Pallister, ed. (New York: Academic Press).